INTERNATIONAL JOURNAL FOR NUMERICAL METHODS IN FLUIDS, VOL. 23, 637–660 (1996)

AN EXTENDED BOUNDARY INTEGRAL EQUATION METHOD FOR THE REMOVAL OF IRREGULAR FREQUENCY EFFECTS

C.-H. LEE, J. N. NEWMAN AND X. ZHU

Department of Ocean Engineering, MIT, Cambridge, MA 02139, U.S.A.

SUMMARY

Numerical techniques for the analysis of wave–body interactions are developed by the combined use of two boundary integral equation formulations. The velocity potential, which is expressed in a perturbation expansion, is obtained directly from the application of Green's theorem (the potential formulation), while the fluid velocity is obtained from the gradient of the alternative form where the potential is represented by a source distribution (the source formulation). In both formulations, the integral equations are modified to remove the effect of the irregular frequencies.

It is well known from earlier works that if the normal velocity is prescribed on the interior free surface, inside the body, an extended boundary integral equation can be derived which is free of the irregular frequency effects. It is shown here that the value of the normal velocity on the interior free surface must be continuous with that outside the body, to avoid a logarithmic singularity in the source strength at the waterline. Thus the analysis must be carried out sequentially in order to evaluate the fluid velocity correctly: first for the velocity potential and then for the source strength.

Computations are made to demonstrate the effectiveness of the extended boundary integral euations in the potential and source formulations. Results are shown which include the added-mass and damping coefficients and the first-order wave-exciting forces for simple three-dimensional bodies and the second-order forces on a tension-leg-platform. The latter example illustrates the importance of removing irregular frequency effects in the context of second-order wave loads.

KEY WORDS: wave–body interaction; integral equation; irregular frequency

1. INTRODUCTION

The interactions of waves with ships and platforms are usually analysed using linearized potential theory, with non-linear effects described by a perturbation expansion in terms of the (small) wave slope. Numerical solutions applicable to bodies of general form can be obtained using the boundary integral equation method, where the velocity potential is represented by distributions of sources and/or normal dipoles on the boundary surfaces of the fluid domain. In a fluid of constant or infinite depth, Green functions which satisfy the linearized free surface condition are known in analytic form and efficient algorithms exist to evaluate these functions. Thus in the first-order analysis it is only necessary to distribute these singularities on the body surface, and after representing this surface in a discretized form, the resulting 'panel methods' are generally more efficient than other numerical approaches.

CCC 0271–2091/96/070637–24

Received September 1995
Revised January 1996

In recent years there has been increased attention to the analysis of second-order wave effects, which are of special importance for large floating platforms in relatively deep water. In particular, the second-order wave forces which are oscillatory at the sum or difference frequency of the first-order waves have been recognized to be the most significant exciting forces for the resonant response of these structures at high and low frequencies respectively. The boundary integral equation formulation utilizing the wave source potential has been successfully applied for these problems since the seminal work of Molin[1] on a bottom-mounted cylinder.

In both the first- and second-order problems, Neumann boundary conditions which prescribe the *normal* velocity of the fluid are specified on the body surface. Two types of integral equations are commonly used. The first, known as the 'potential formulation', is derived by applying Green's theorem to the unknown velocity potential and the wave source potential; the potential is then expressed by distributions of both sources and normal dipoles on the body surface. In the alternative 'source formulation' the velocity potential is represented by a distribution of wave sources alone on the body surface. The integral equation for the source formulation can be formally derived by applying Green's theorem not only in the fluid domain but also in the domain interior to the body surface (Reference 2, §58).

Both of these formulations lead to Fredholm integral equations of the second kind, which are preferable to the first-kind equations from the computational viewpoint because of their diagonal dominance. An important relation which exists between the two formulations is that the kernel of one is the transpose of the other. Restricting our attention to the problems where the unsteady motion is harmonic, the boundary condition on the free surface is of the mixed type involving a linear combination of the potential and its normal derivative. This free surface condition is homogeneous in the case of the first-order velocity potential but inhomogeneous for the second-order potential. In the latter case the inhomogeneous term appears only as a forcing in the integral equations because the wave source potential itself satisfies the homogeneous free surface condition. Thus the integral equations have the same kernel for the first- and second-order problems.

One disadvantage of these methods, for bodies which intersect the free surface, is that a discrete spectrum of 'irregular frequencies' exists where the solutions of the boundary integral equations either do not exist or are non-unique. This is a consequence of the fact that the Green function satisfies the free surface condition everywhere on the plane of the free surface, both outside and inside the body. The irregular frequencies coincide with the eigenfrequencies of non-physical wave motions inside the body, where the same free surface condition is imposed on the interior free surface and a homogeneous Dirichlet boundary condition is applied on the body surface.

The connection between the irregular frequencies and the interior Dirichlet problem follows by noting that this problem can be solved in general by either the potential or source formulation. However, the corresponding fluid motion inside the body, subject to a Dirichlet condition, would have a set of resonance frequencies at which non-trivial homogeneous solutions exist. The potential and source formulations for the exterior boundary value problem break down at the same frequencies owing to the relation of their kernels to that of the integral equation for the interior Dirichlet problem. At the irregular frequencies the Fredholm determinants of the two formulations vanish and thus the solutions must be either non-unique or non-existent. The same set of irregular frequencies applies to the potential and source formulations and to the second-order solution, since each of the corresponding integral equations has the same kernel or its transpose.

Numerical solutions for bodies of practical shape require that the body surface be discretized, usually in terms of small flat rectangular or triangular 'panels'. In the low-order panel method the velocity potential and source strength are discretized in a corresponding manner, with constant values on each panel. The continuous integral equation is then replaced by a linear system of equations for the unknown potential or source strength on each panel.

In the discrete problem the condition number of the linear system increases near the irregular frequencies, indicating that the system is ill-conditioned in the neighbourhoods of the irregular frequencies.[3] The numerical solutions are erroneous in the vicinity of the irregular frequencies. The bandwidth of the polluted solution may be reduced arbitrarily by using a finer discretization of the boundary surface. However, it is impractical to reduce the bandwidth in this manner, since the computational burden increases with the increasing number of panels; this difficulty is aggravated by the fact that in most cases it is not possible to predict the location of the irregular frequencies. Thus it is necessary to develop modified integral equations which avoid the effects of the irregular frequencies in practical applications.

Ohmatsu[4] derived a modified form of the source formulation, where the eigenmodes of the interior Dirichlet problem are suppressed, by imposing a Neumann condition on the interior free surface. In this formulation the interior free surface is included as part of the boundary on which the wave sources are distributed. The computational results, performed with the 'rigid lid' condition of zero normal velocity on the interior free surface, confirmed that the velocity potential was free of the irregular frequency effects. In Section 3 we will discuss the details of the behaviour of the source strength and its effect on the evaluation of the fluid velocity. Kleinman[5] derived a counterpart for the potential formulation and also proved the uniqueness of the solution. We refer to these two modified formulations as 'extended boundary integral equations'. Their kernels are the transpose of each other, as in the case of the unmodified formulations. Thus the uniqueness of the solution of one formulation implies the uniqueness of the other.

Ogilvie and Shin[6] placed a localized wave source on the interior free surface and removed the first irregular frequency for simple heaving bodies. Ursell[7] showed that a sequence of singularities is necessary to remove more than the first irregular frequency from the integral equation. Zhu[8] extended this method to practical three-dimensional problems by distributing wave sources and their derivatives on the interior free surface. However, the success of this method was found to be sensitive to the body shape, the wave frequency and strengths and locations of the singularities.

Following the theory of Burton and Miller[9] in acoustics, Kleinman[5] and Lee and Sclavounos[3] derived a modified integral equation for the potential formulation from a linear combination of the Green' integral equation and its normal derivative. If the complex constant of proportionality has non-zero imaginary part, there is no non-trivial homogeneous solution. This implies that no interior eigenmode exists which satisfies a mixed boundary condition on the body surface with the same proportionality constant. This method was applied to three-dimensional problems by Lee and Sclavounos,[3] who showed that it is successful in removing all irregular frequencies from the velocity potential. Computationally, however, the direct evaluation of the hypersingular integral accounting for the normal velocity due to the normal dipole distributed over the panel causes substantial discretization error. The conditioning of the discrete system of the modified equation is worse than that of the unmodified Green' equation, except in the vicinity of the irregular frequencies. As a result, the convergence rate of the solution with respect to the discretization is much slower than that of the unmodified equation.

In this paper we study the extended boundary integral equations suitable for both the first- and second-order boundary value problems. In the computation, the velocity potential is evaluated first from the potential formulation and then the fluid velocity is evaluated from the source formulation. The motivation for this sequential use of two formulations is twofold. First, as noted by Zhao and Faltinsen,[10] the fluid velocity is not predicted accurately close to the body surface by the potential formulation and thus we have to resort to the source formulation in the low-order panel method. On the other hand, as will be discussed in Section 3, the source strength of the extended boundary integral equation is logarithmically singular at the waterline unless the value specified for the vertical velocity on the interior free surface is continuous with the vertical velocity of the exterior flow at the

waterline. To avoid this difficulty, the required vertical velocity on the interior free surface for the source formulation is obtained using the free surface condition and the exterior velocity potential near the waterline, where the latter quantity is computed from the potential formulation.

In Sections 2 and 3 the extended boundary integral equations for the potential and source formulations are derived. The proper Neumann condition on the interior free surface for the source formulation is discussed in Section 3. In Section 4 the first- and second-order hydrodynamic pressure forces are computed using extended boundary integral equations which are discretized based on the low-order panel method. Illustrative results are presented for the added-mass and damping coefficients and wave-exciting forces acting on a circular cylinder and Wigley hull, and for the second-order sum-frequency exciting force on a tension-leg-platform (TLP). The irregular frequency effects are removed from all these results. Comparisons are made between the results based on the unmodified and extended boundary integral equations. Negligible differences are found between the two results over a broad range of frequencies away from the irregular frequencies. Also presented is the fluid velocity on the surface of a cylinder in order to show the importance of the proposed Neumann condition for the source formulation.

2. PROBLEM STATEMENT AND POTENTIAL FORMULATION

Cartesian co-ordinates $\mathbf{x} = (x, y, z)$ are defined with $z = 0$ the plane of the undisturbed free surface and $z < 0$ the fluid domain, as shown in Figure 1. Irrotational flow is assumed and the velocity potential is represented by a perturbation expansion in terms of a small parameter (i.e. the incident wave slope).

Our objective is to evaluate the first- and second-order velocity potentials corresponding to the first two terms of the perturbation expansion, using boundary integral equations which are modified to avoid introducing irregular frequency effects. A time-harmonic dependence applies throughout, permitting the use of a complex notation for all oscillatory quantities, including the velocity potential. Thus the real part of the product of all complex quantities with the factor $e^{i\omega t}$ is understood hereafter, where ω denotes an appropriate radian frequency. In the first-order analysis ω is the frequency of the incident waves. In the second-order analysis ω denotes the sum or difference of the frequencies of two linear solutions.

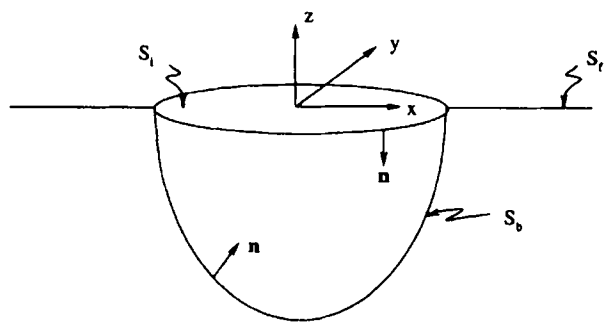

Figure 1. Cartesian co-ordinate system

Since the occurrence of the irregular frequencies is associated with the interior Dirichlet problem, their effects in water of infinite or finite depth are similar. Only the former case is considered here and the incident wave is represented by the first-order velocity potential

$$\phi_I = \frac{igA}{\omega} e^{\nu z - i\nu(x\cos\beta + y\sin\beta)}, \tag{1}$$

where g is the gravitational constant, A is the wave amplitude, $\nu = \omega^2/g$ is the wave number and β is the propagation angle of the incident waves relative to the positive x-axis. The corresponding definition of the second-order incident wave due to the interaction of two first-order incident waves is given in Appendix I.

The remainder of the velocity potential due to the presence of the body will be determined here. It may be decomposed into several components, but they are subject to one canonical form of the boundary conditions. Thus in the following discussion it is sufficient to consider a representative velocity potential ϕ which satisfies Laplace's equation in the fluid domain. The boundary conditions include the free surface condition

$$-\omega^2\phi + g\frac{\partial\phi}{\partial z} = q_f \quad \text{on} \quad z = 0, \tag{2}$$

a Neumann condition which prescribes the normal velocity on the mean position of the body surface,

$$\frac{\partial\phi}{\partial n} = q_b \quad \text{on} \quad S_b, \tag{3}$$

and vanishing of the fluid motion at large depths,

$$\phi \to 0 \quad \text{as} \quad z \to -\infty. \tag{4}$$

In the far field the first-order velocity potential is subject to a Sommerfeld radiation condition, i.e. the waves due to the presence of the body are outgoing at large horizontal distances from the body. Following Molin,[1] the far-field behaviour of the second-order potential includes both outgoing 'free' waves, which also satisfy a conventional radiation condition, and 'locked' waves which are in phase with q_f. The forcing functions q_f and q_b depend on the component potentials as listed in Appendix I.

Integral equations suitable for evaluating the potential ϕ may be derived by applying Green's theorem to the volume of fluid in the domain which is bounded by S_b, S_f, and a closure surface which is in the far field and at large depths below the free surface. For this purpose we use the Green function

$$G(\mathbf{x};\boldsymbol{\xi}) = \frac{1}{r} + \frac{1}{r'} + 2\nu\int_0^\infty dk\,\frac{e^{k(z+\zeta)}}{k-\nu}J_0(kR), \tag{5}$$

where

$$r^2 = (x-\xi)^2 + (y-\eta)^2 + (z-\eta)^2, \tag{6}$$

$$r'^2 = (x-\xi)^2 + (y-\eta)^2 + (z+\zeta)^2 \tag{7}$$

(see Reference 11, equation 13.17). This Green function is the velocity potential due to a point source with oscillatory strength located at the point (ξ, η, ζ). It vanishes for large depths and satisfies the homogeneous form of (2) on the entire plane $z = 0$ which includes the free surface exterior to the body and its extension within the body. The contour of integration in (5) is indented above the pole and with this definition the Green function satisfies the Sommerfeld radiation condition in the far field.

Green's theorem yields a Fredholm integral equation for the unknown $\phi(\mathbf{x})$ over the domain S_b,

$$2\pi\phi(\mathbf{x}) + \iint_{S_b} \phi(\boldsymbol{\xi}) \frac{\partial G(\mathbf{x}; \boldsymbol{\xi})}{\partial n_{\boldsymbol{\xi}}} d\boldsymbol{\xi} = \iint_{S_b} q_b(\boldsymbol{\xi}) G(\mathbf{x}; \boldsymbol{\xi}) d\boldsymbol{\xi} + F(\mathbf{x}), \tag{8}$$

where

$$F(\mathbf{x}) = \frac{1}{g} \iint_{S_f} q_f(\boldsymbol{\xi}) G(\mathbf{x}; \boldsymbol{\xi}) d\boldsymbol{\xi}. \tag{9}$$

For later use we define the normal derivative of (9) by

$$F_n(\mathbf{x}) = \frac{1}{4\pi g} \iint_{S_f} q_f(\boldsymbol{\xi}) \frac{\partial G(\mathbf{x}; \boldsymbol{\xi})}{\partial n_x} d\boldsymbol{\xi}. \tag{10}$$

The normal vector $\mathbf{n}$ points out of the fluid domain and S_f denotes the free surface exterior to the body.

Note that since the Green function satisfies the homogeneous form of (2), the only contribution to (8) from the free surface is associated with the forcing function q_f. With the far-field conditions as stated above, there is no contribution to (8) from the surface integral which provides closure in the far field.

While it is generally assumed that solutions of the boundary value problem for the potential ϕ are unique, in the unbounded fluid domain exterior to the body, it can be shown that non-trivial homogeneous solutions of (8) exist at the irregular frequencies. The existence of these homogeneous solutions is associated with the non-physical portion of the free surface domain interior to the body in the definition of the Green function (5). To verify this statement, we note that if Green's theorem is applied to an artificial interior potential and G in the interior domain, the result is an integral equation identical with (8) except for the direction of the normal vector (i.e. 2π should be replaced by -2π) and $F(\mathbf{x}) = 0$. Non-trivial solutions of this interior problem exist at discrete eigenfrequencies, not only for the physical problem of 'sloshing' or standing waves, where a homogeneous Neumann condition is applied on S_b, but also for the corresponding interior Dirichlet problem where the boundary condition (3) is replaced by ϕ. In the latter case the left-hand side of (8) vanishes and thus the integral on the right-hand side vanishes, implying that a distribution of normal velocity $q_b = \partial\phi/\partial n$ exists which is orthogonal to the Green function on the body surface at these eigenfrequencies. Thus the corresponding exterior potential, with this distribution of normal velocity on the body and with the homogeneous free surface condition, is a non-trivial homogeneous solution of (8).

A simple way to extend the integral equation (8) is to apply Green's theorem also to a field point $\mathbf{x}$ interior to S_b, where

$$\iint_{S_b} \phi(\boldsymbol{\xi}) \frac{\partial G(\mathbf{x}; \boldsymbol{\xi})}{\partial n_{\boldsymbol{\xi}}} d\boldsymbol{\xi} = \iint_{S_b} q_b(\boldsymbol{\xi}) G(\mathbf{x}; \boldsymbol{\xi}) d\boldsymbol{\xi} + F(\mathbf{x}). \tag{11}$$

Equation (8) supplemented by the first-kind integral equation (11) has no non-trivial homogeneous solution unless all $\mathbf{x}$ in (11) coincide with nodal points of the interior Dirichlet eigensolutions. The latter possibility, however, can be avoided easily in practice by enforcing equation (11) at a sufficiently large number of interior points. Further discussion on the combined use of the second- and first-kind integral equations can be found in the paper by Schenck,[12] who applied the technique to the acoustic radiation problem. This technique has also been applied to wave–body interactions by Lau and Hearn.[13]

The linear system of equations which results from discretization and collocation of (8), augmented by (11), is an overdetermined system of algebraic equations which requires special numerical techniques for its solution. This is not a convenient form to solve, especially when we employ both the potential and source formulations, since the latter results in a square system of equations as is discussed in the next section.

In order to derive a square system of equations, we first consider a boundary value problem in the interior domain. Consider an interior velocity potential ψ, subject to

$$\frac{\partial \psi}{\partial n} = 0 \quad \text{on} \quad S_i, \tag{12}$$

$$\psi = 0 \quad \text{on} \quad S_b. \tag{13}$$

In (12), S_i denotes the interior free surface and on this surface the normal vector is directed towards the negative z-axis. From Green's first identity

$$\iiint_V |\nabla \psi|^2 \mathrm{d}V = \iint_{S_b+S_i} \psi \frac{\partial \psi^*}{\partial n} \mathrm{d}S, \tag{14}$$

where the superscript asterisk denotes the complex conjugate, and by the usual uniqueness proof of simple potential flows there can be no non-trivial solution ψ subject to the boundary conditions (12) and (13).

Suppose the same ψ is expressed by a normal dipole distribution over the closed surface with the understanding that the dipole strength is also trivial. It takes the form

$$\psi(\mathbf{x}) = \iint_{S_b+S_i} \mu(\boldsymbol{\xi}) \frac{\partial G(\mathbf{x}; \boldsymbol{\xi})}{\partial n_{\boldsymbol{\xi}}} \mathrm{d}\boldsymbol{\xi} \quad \text{for} \quad \mathbf{x} \in V. \tag{15}$$

From the conditions of (13) and (12), we obtain a pair of equations

$$2\pi\mu(\mathbf{x}) + \iint_{S_b+S_i} \mu(\boldsymbol{\xi}) \frac{\partial G(\mathbf{x}; \boldsymbol{\xi})}{\partial n_{\boldsymbol{\xi}}} \mathrm{d}\boldsymbol{\xi} = 0 \quad \text{for} \quad \mathbf{x} \in S_b, \tag{16}$$

$$-4\pi\mu(\mathbf{x}) + \iint_{S_b+S_i} \mu(\boldsymbol{\xi}) \frac{\partial G(\mathbf{x}; \boldsymbol{\xi})}{\partial n_{\boldsymbol{\xi}}} \mathrm{d}\boldsymbol{\xi} = 0 \quad \text{for} \quad \mathbf{x} \in S_i, \tag{17}$$

which cannot have a non-trivial solution. Here the free term in (16) is derived in the conventional manner from the dipole singularity at the point $\mathbf{x} \to \boldsymbol{\xi}$, but the free term in (17) is different, as noted below.

In the vicinity of the singular point on S_i, G is of the form (Reference 14, equation 5)

$$G(\mathbf{x}; \boldsymbol{\xi}) = \frac{1}{r} + \frac{1}{r'} - 2\nu \mathrm{e}^{\nu(z+\zeta)}[\log(r' + |z+\zeta|) + (\gamma - \log 2) + r'] + O(r'^2 \log r'), \tag{18}$$

where $\gamma = 0{\cdot}577\ldots$ is Euler's constant. Thus

$$\lim_{z \to 0-} \partial G(\mathbf{x}; \xi, \eta, 0)/\partial z = \lim_{z \to 0-} \partial(1/r + 1/r')/\partial z + O(1/r') \tag{19}$$

and the leading-order term $-2z/r^3$ tends to a delta function with area 4π. The corresponding value for the normal dipole is identically zero:

$$\lim_{z \to 0-} \partial G(\mathbf{x}; \xi, \eta, \zeta)/\partial \zeta|_{\zeta=0} = 0. \tag{20}$$

From (19) and (20) the following relations are obtained and applied in the derivation of (17):

$$\begin{aligned}\lim_{z\to 0-}\iint_{S_i}\mu(\xi)\frac{\partial G(\mathbf{x};\xi)}{\partial n_{\mathbf{x}}}\mathrm{d}\xi &= 4\pi\mu(\mathbf{x})+\iint_{S_i}\mu(\xi)\frac{\partial G(\mathbf{x};\xi)}{\partial n_{\mathbf{x}}}\mathrm{d}\xi\\ &= -4\pi\mu(\mathbf{x})-\nu\iint_{S_i}\mu(\xi)G(\mathbf{x};\xi)\mathrm{d}\xi\\ &= -4\pi\mu(\mathbf{x})+\iint_{S_i}\mu(\xi)\frac{\partial G(\mathbf{x};\xi)}{\partial n_{\xi}}\mathrm{d}\xi\\ &= -4\pi\mu(\mathbf{x})+\lim_{z\to 0-}\iint_{S_i}\mu(\xi)\frac{\partial G(\mathbf{x};\xi)}{\partial n_{\xi}}\mathrm{d}\xi.\end{aligned} \tag{21}$$

Equations (16) and (17) are derived by considering the trivial interior solution and corresponding dipole moment μ. The comparison between these equations and equations (8) and (11) suggests the following pair of equations which may be added to (8) and (11) to prescribe homogeneous solutions:

$$\iint_{S_i}\phi'(\xi)\frac{\partial G(\mathbf{x};\xi)}{\partial n_{\xi}}\mathrm{d}\xi = 0 \quad \text{for} \quad \mathbf{x}\in S_b, \tag{22}$$

$$-4\pi\phi'(\mathbf{x})+\iint_{S_i}\phi'(\xi)\frac{\partial G(\mathbf{x};\xi)}{\partial n_{\xi}}\mathrm{d}\xi = 0 \quad \text{for} \quad \mathbf{x}\in S_i. \tag{23}$$

However, (22) and (23) can be derived in a more direct manner. Consider the potential ϕ' when a disc of shape S_i on the calm free surface has no normal velocity. This physically trivial problem, with the solution $\phi'=$ constant, may be cast into an integral equation for the unknown ϕ' subject to the homogeneous Neumann condition on S_i. Thus equation (23) is obtained from the vertical derivative of the Green integral equation utilizing the jump conditions in (21). We find that $\phi'=0$ is one solution of (23). Owing to the uniqueness of the solution of the exterior boundary value problem[15] and the geometry devoid of the interior free surface, it follows that (23) has no non-trivial solution. Equation (22) is a consequence of the trivial solution of (23) and, together, they form an overdetermined system.

Combining (22) and (23) with (8) and (11) we obtain the following extended boundary integral equation in the potential formulation:

$$2\pi\phi(\mathbf{x})+\iint_{S_b+S_i}\phi(\xi)\frac{\partial G(\mathbf{x};\xi)}{\partial n_{\xi}}\mathrm{d}\xi = \iint_{S_b}q_b(\xi)G(\mathbf{x};\xi)\mathrm{d}\xi+F(\mathbf{x}) \quad \text{for} \quad \mathbf{x}\in S_b, \tag{24}$$

$$-4\pi\phi(\mathbf{x})+\iint_{S_b+S_i}\phi(\xi)\frac{\partial G(\mathbf{x};\xi)}{\partial n_{\xi}}\mathrm{d}\xi = \iint_{S_b}q_b(\xi)G(\mathbf{x};\xi)\mathrm{d}\xi+F(\mathbf{x}) \quad \text{for} \quad \mathbf{x}\in S_i. \tag{25}$$

Here ϕ' on S_i is replaced by ϕ for the sake of the compactness of the expression. The uniqueness of the solution of (24) and (25) follows directly from that of (16) and (17), because their kernels are identical. Therefore ϕ and ϕ', the solutions of the two separate uniquely solvable integral equations, are the only solution of the extended boundary integral equation.

Despite the uniqueness of the solution of the continuous problem, a restriction applied to (8) and (11) is also applicable to (24) and (25) if we discretize the latter based on the low-order panel method and collocate at discrete points on S_i. Thus the collocation points on S_i in (25) should not coincide identically with the nodal points of the Dirichlet eigenmodes. In order to see this, note that if the collocation points in (25) are the same as $\mathbf{x}$ of (11), part of the influence coefficients of (24) and (25) is the same as that of (8) and (11). In this case the erroneous solution of (8) and (11) is also the solution of ϕ on S_b of the discrete system of (24) and (25), assuming the latter has a unique solution.

This degenerate situation can be avoided, as in (11), by using a sufficiently large number of collocation points within a typical wavelength of the Dirichlet eigenmodes. Thus the discretization on S_i, like on the physical surface S_b, should depend on the wave frequency.

3. SOURCE FORMULATION

The external velocity potential ϕ may also be expressed as a distribution of sources only on S_b. Following the formal derivation given by Lamb (Reference 2, §58), the source strength is defined by the difference of the interior and exterior velocities normal to S_b, where the latter is prescribed by (2). The interior potential is assumed to have continuous value to the exterior potential on S_b and to satisfy the homogeneous free surface condition. When the interior problem defined in this way has Dirichlet eigensolutions, the interior normal velocity and thus the source strength are not uniquely determined at the irregular frequencies. On the other hand, we have shown that the interior problem with the mixed boundary conditions (12) and (13) has only the trivial homogeneous solution. Therefore the interior solution can be determined uniquely by imposing a Neumann condition on S_i instead of the homogeneous free surface condition. With this condition for the interior potential we derive the extended boundary integral equation for the source formulation following the procedure described by Ohmatsu.[4]

We first consider exterior velocity potentials ϕ subject to (2), (4) and the radiation condition. For $\mathbf{x}$ in the fluid domain, Green's theorem yields

$$4\pi\phi(\mathbf{x}) + \iint_{S_b} \phi(\boldsymbol{\xi}) \frac{\partial G(\mathbf{x};\boldsymbol{\xi})}{\partial n_{\boldsymbol{\xi}}} \mathrm{d}\boldsymbol{\xi} = \iint_{S_b} \frac{\partial \phi(\boldsymbol{\xi})}{\partial n} G(\mathbf{x};\boldsymbol{\xi})\mathrm{d}\boldsymbol{\xi} + F(\mathbf{x}). \tag{26}$$

Next we consider an interior potential which is continuous to the exterior potential:

$$\psi(\mathbf{x}) = \phi(\mathbf{x}) \quad \text{on} \quad S_b. \tag{27}$$

The interior potential ψ is uniquely determined by imposing the boundary condition

$$\frac{\partial \psi(\mathbf{x})}{\partial n} = -V(\mathbf{x}) \quad \text{on} \quad S_i. \tag{28}$$

The function $V(\mathbf{x})$ will be prescribed in an appropriate manner below. Again, for $\mathbf{x}$ in the fluid domain we apply Green's theorem in the interior domain to give

$$\iint_{S_b} \psi(\boldsymbol{\xi}) \frac{\partial G(\mathbf{x};\boldsymbol{\xi})}{\partial n_{\boldsymbol{\xi}}} \mathrm{d}\boldsymbol{\xi} = \iint_{S_b} \frac{\partial \psi(\boldsymbol{\xi})}{\partial n} G(\mathbf{x};\boldsymbol{\xi})\mathrm{d}\boldsymbol{\xi} + \iint_{S_i} \left(\nu\psi(\boldsymbol{\xi}) + \frac{\partial \psi(\boldsymbol{\xi})}{\partial n} \right) G(\mathbf{x};\boldsymbol{\xi})\mathrm{d}\boldsymbol{\xi}. \tag{29}$$

Upon subtracting (29) from (26), we have

$$\phi(\mathbf{x}) = \iint_{S_b+S_i} \sigma(\boldsymbol{\xi}) G(\mathbf{x};\boldsymbol{\xi})\mathrm{d}\boldsymbol{\xi} + \frac{1}{4\pi} F(\mathbf{x}), \tag{30}$$

where the source strength $\sigma(\mathbf{x})$ is defined as

$$\sigma(\mathbf{x}) = \begin{cases} \dfrac{1}{4\pi}\left(\dfrac{\partial \phi(\mathbf{x})}{\partial n} - \dfrac{\partial \psi(\mathbf{x})}{\partial n} \right), & \mathbf{x} \in S_b, \\ \dfrac{-1}{4\pi}\left(\nu\psi(\mathbf{x}) + \dfrac{\partial \psi(\mathbf{x})}{\partial n} \right), & \mathbf{x} \in S_i. \end{cases} \tag{31}$$

Equation (30) has been derived for $\mathbf{x}$ exterior to S_b. However, it is also valid for $\mathbf{x}$ on or interior to S_b, since the potential due to a continuous source distribution is continuous across the surface.[16] In the latter case $\phi(\mathbf{x})$ should be replaced by $\psi(\mathbf{x})$ in (30).

The integral equation for the source strength is obtained from the normal derivative of (30) on the body and interior free surface with conditions (3) and (28):

$$2\pi\sigma(\mathbf{x}) + \iint_{S_b+S_i} \sigma(\boldsymbol{\xi}) \frac{\partial G(\mathbf{x};\boldsymbol{\xi})}{\partial n_{\mathbf{x}}} d\boldsymbol{\xi} = q_b(\mathbf{x}) - F_n(\mathbf{x}) \quad \text{for} \quad \mathbf{x} \in S_b, \tag{32}$$

$$-4\pi\sigma(\mathbf{x}) + \iint_{S_b+S_i} \sigma(\boldsymbol{\xi}) \frac{\partial G(\mathbf{x};\boldsymbol{\xi})}{\partial n_{\mathbf{x}}} d\boldsymbol{\xi} = -V(\mathbf{x}) - F_n(\mathbf{x}) \quad \text{for} \quad \mathbf{x} \in S_i, \tag{33}$$

where $F_n(\mathbf{x})$ is defined by (10). The free term in (33) accounts for the jump due to the Rankine source and its image above the free surface, as discussed in the previous section.

Equations (32) and (33) are the desired extended boundary integral equation for the source formulation. Note that the kernel of these equations is the transpose of the pair of equations (24) and (25). It follows that there are no non-trivial homogeneous solutions of (32) and (33).

In the conventional unmodified source formulation, which suffers from the irregular frequency effect, the interior flow satisfies the condition (27) on S_b but the homogeneous free surface condition instead of (28). With these conditions for the interior potential $\psi'(\mathbf{x})$ we have

$$\phi(\mathbf{x}) = \iint_{S_b} \sigma'(\boldsymbol{\xi}) G(\mathbf{x};\boldsymbol{\xi}) d\boldsymbol{\xi} + \frac{1}{4\pi} F(\mathbf{x}). \tag{34}$$

The source strength in (34), which is defined by

$$\sigma'(\mathbf{x}) = \frac{1}{4\pi}\left(\frac{\partial\phi(\mathbf{x})}{\partial n} - \frac{\partial\psi'(\mathbf{x})}{\partial n}\right), \tag{35}$$

differs from that of (31) on S_b because of the different interior flow.

The potential $\phi(\mathbf{x})$ in (34) is subject to (2), (4) and the radiation condition. The remaining boundary condition (3) on S_b is imposed through the normal derivative of (34):

$$2\pi\sigma'(\mathbf{x}) + \iint_{S_b} \sigma'(\boldsymbol{\xi}) \frac{\partial G(\mathbf{x};\boldsymbol{\xi})}{\partial n_{\mathbf{x}}} d\boldsymbol{\xi} = \frac{\partial\phi(\mathbf{x})}{\partial n} - F_n(\mathbf{x}). \tag{36}$$

Since equations (30) and (34) express the solution of the same boundary value problem, it follows that

$$\iint_{S_b} \frac{\partial\psi(\boldsymbol{\xi})}{\partial n} G(\mathbf{x};\boldsymbol{\xi}) d\boldsymbol{\xi} + \iint_{S_i} [\nu\psi(\boldsymbol{\xi}) - V(\xi,\eta)] G(\mathbf{x};\boldsymbol{\xi}) d\boldsymbol{\xi} = \iint_{S_b} \frac{\partial\psi'(\boldsymbol{\xi})}{\partial n} G(\mathbf{x};\boldsymbol{\xi}) d\boldsymbol{\xi}. \tag{37}$$

This relation can be confirmed by applying Green's theorem separately to ψ and ψ' with the appropriate boundary conditions for these interior potentials specified above.

As yet we have not restricted the normal velocity $V(\mathbf{x})$ in (28). This will be determined based on the following consideration. We restrict our attention to bodies which intersect the free surface perpendicularly. The line of the intersection is denoted by C_w hereafter. We first notice that the vertical derivative of the interior potential, $\partial\psi/\partial z$, on S_b is the same as that of the exterior potential, $\partial\phi/\partial z$, owing to the condition (27), while $\partial\psi/\partial z$ on S_i is specified by $V(\mathbf{x})$. In Appendix II it is shown that if $\partial\psi/\partial z$ is not continuous across the intersection C_w, the interior potential has a weak singularity such that the corresponding source strength (31) has a logarithmic singularity at C_w. With this singularity in the source strength the surface integral over S_b is shown to be unbounded as $\mathbf{x}$

approaches C_w, when we evaluate the vertical tangential component of the fluid velocity from the gradient of the extended boundary integral equation (30). In order to avoid this difficulty, $V(\mathbf{x})$ should take the same value as $\partial\phi/\partial z$ at C_w:

$$V(x, y, 0) = \nu\phi(x, y, 0) + \frac{1}{g} q_f \quad \text{on} \quad C_w, \tag{38}$$

where we use the free surface condition (2) for $\partial\phi/\partial z$. Since $V(\mathbf{x})$ can be specified properly only after the exterior potential is known, we obtain the latter from the solution of the potential formulation (24) and (25) before proceeding with the solution of the source formulation (32) and (33).

It is interesting to note that the surface intergals for the velocity potential (26) are always bounded, despite the singular behaviour of the source strength. More detailed discussion is provided in Appendix II.

4. NUMERICAL RESULTS

Numerical results will be presented here to illustrate the use of the extended boundary integral equations. For this purpose the panel program WAMIT (Wave Analysis MIT) is used, with appropriate modifications to extend the computational domain into the interior free surface. Details on WAMIT were reported in References 17 and 18.

The first-order results include the added-mass and damping coefficients α_{ij} and β_{ij} defined as

$$\alpha_{ij} - \frac{1}{\omega}\beta_{ij} = \rho \int\int_{S_b} n_i \phi_j \mathrm{d}S, \tag{39}$$

where ϕ_j is the radiation potential due to the jth mode of motion of the body, and the first-order wave-exciting force defined as

$$\mathbf{F}^{(1)} = -\mathrm{i}\omega\rho \int\int_{S_b} (\phi_I^{(1)} + \phi_S^{(1)})\mathbf{n}\mathrm{d}S. \tag{40}$$

In (40) and subsequent expressions the force and moment are included in the generalized vector $\mathbf{F}$ with the definition of the generalized normal vector $\mathbf{n}$ to include $\mathbf{x} \times \mathbf{n}$ for the rotational modes.

The second-order results include the sum-frequency wave-exciting force, which consists of two separate components

$$\mathbf{F}^{(2)} = \mathbf{F}_p + \mathbf{F}_q. \tag{41}$$

Here $\mathbf{F}_p$ and $\mathbf{F}_q$ account for the hydrodynamic pressure forces due to the unsteady second-order potential and the quadratic interaction of the first-order solutions respectively. The former takes the form

$$\mathbf{F}_p = -\mathrm{i}\omega\rho \int\int_{S_b} (\phi_I^{(2)} + \phi_S^{(2)})\mathbf{n}\mathrm{d}S \tag{42}$$

and the latter takes a relatively simple form for a fixed body,

$$\mathbf{F}_q = \tfrac{1}{2}\rho g \int_{C_w} \mathbf{n}\zeta^2(1 - n_z^2)^{-1/2}\mathrm{d}l - \tfrac{1}{2}\rho \int\int_{S_b} \mathbf{n}\nabla\phi^{(1)} \cdot \nabla\phi^{(1)}\mathrm{d}S, \tag{43}$$

where ζ is the first-order free surface elevation or 'run-up'. When the body oscillates, the corresponding expression for $\mathbf{F}_q$ is more complicated. A complete account of the effects of the body motion on the second-order quadratic force can be found in Reference 19. An alternative expression for $\mathbf{F}_p$ can be derived from Green's theorem by following the method proposed by Faltinsen and Løken,[20] Lighthill[21] and Molin.[1] This alternative expression takes the form

$$\mathbf{F}_p = -i\rho\omega\left[\iint_{S_b}\left(\boldsymbol{\psi}\frac{\partial\phi_S^{(2)}}{\partial n} + \phi_I^{(2)}\mathbf{n}\right)dS + \frac{1}{g}\iint_{S_f} q_f\boldsymbol{\psi}dS\right]. \tag{44}$$

Here $\boldsymbol{\psi}$ is a vector form of the radiation potentials which is often referred to as the 'assisting potential'.

The radiation and scattered potentials in (39)–(44) are evaluated from the potential formulation (24) and (25). On the other hand, the fluid velocity in (43) and the velocity potential and its derivatives in q_f are obtained from the source formulation (32) and (33). The source formulation is also used for the evaluation of the assisting potential and its derivatives in the modified form of the free surface integral in (44). The free surface integral in (44) is modified using the Gauss theorem in order to avoid the double spatial derivative of the first-order potentials in q_f shown by equations (46) and (47) in Appendix I.

Figure 2 shows two discretizations which are used in the computation for a cylinder with the draft–radius ratio equal to 0·5. The discretizations are the same on S_b but are different on S_i. The discretization (a) is obtained using an algorithm for automatic discretization of the interior free surface developed by Zhu,[8] while (b) has a more systematic pattern. It is found that the accuracy of the numerical solution is not sensitive to the discretization on S_i in potential formulation. The added-mass and damping coefficients and the first-order wave exciting forces obtained using the two discretizations are practically identical. On the other hand, it is important to impose the continuity of the vertical fluid velocity from S_b (exterior flow) to S_i (interior flow) across the waterline to suppress the singular behaviour of the source strength near C_w. Thus only the discretization (b) is used for the source formulation.

Figures 3 and 4 show the added-mass and damping coefficients and the wave exciting forces on the cylinder for the surge and heave modes respectively. The comparisons are made between the results from the unmodified and the extended boundary integral equations. S_b is discretized with 288 panels and S_i with 56 panels as shown in Figure 2(a). (In the computations, two planes of symmetry are utilized and the unknowns are reduced to one-quarter of the total number of panels.) The results demonstrate the effectiveness of the extended boundary integral equation for the removal of the irregular frequencies with a relatively small increment of the unknowns. Similar results are shown in

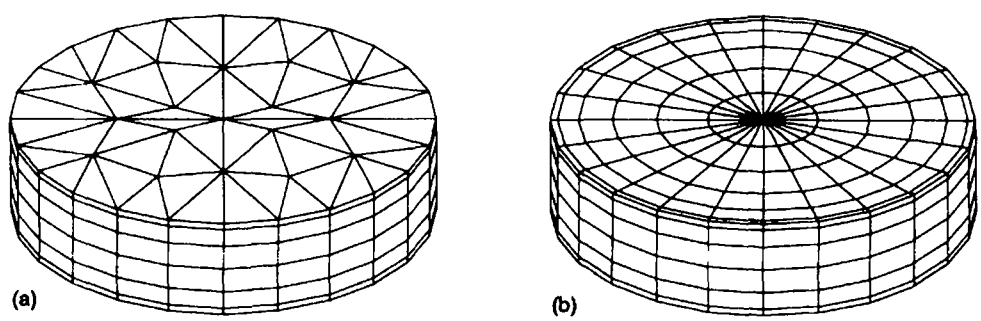

Figure 2. Discretizations of the cylinder. Two types of discretization on S_i are used in the computation

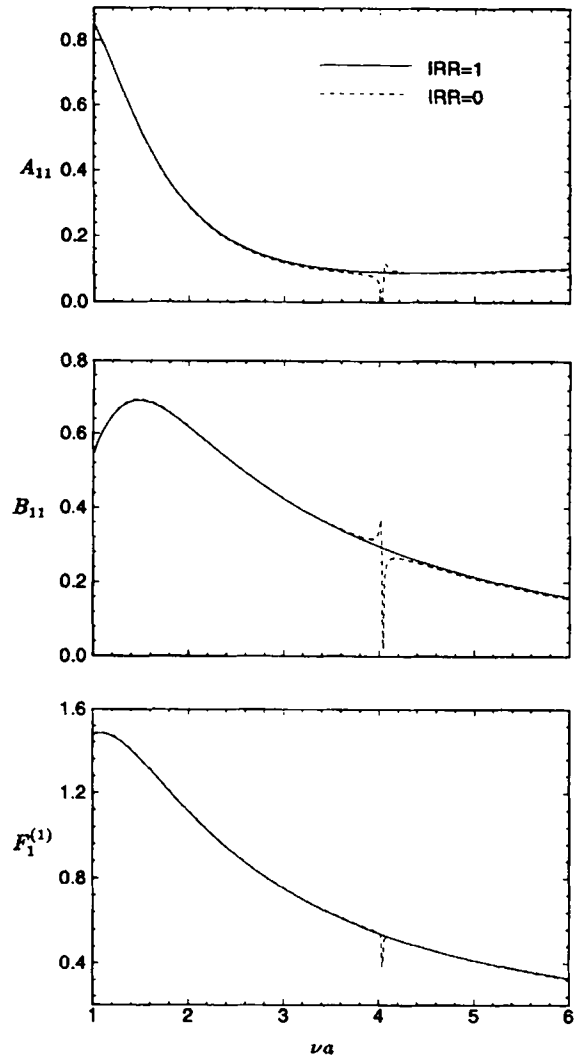

Figure 3. Surge added mass and damping coefficients and modulus of the linear exciting force on the cylinder as functions of non-dimensional wave νa. They are non-dimensionalized by ρa^3, $\rho a^3 \omega$ and $\rho g A a^2$ respectively. Here a is the cylinder radius, ρ the water density, ω the wave frequency, A the incident wave amplitude and g the gravitational acceleration. Comparisons are made between the results from the unmodified (IRR = 0) and extended (IRR = 1) boundary integral equations

Figure 6, where the heave added mass and damping coefficients and the exciting force for the Wigley ship hull shown in Figure 5 are plotted. The discretization of this hull is shown in Figure 5 with 1152 panels on S_b and 220 on S_i.

Next we examine the computational results based on the source formulation. Three results are compared for this purpose. They are from the unmodified equation, from the extended equation with the condition $V(\mathbf{x}) = 0$ on S_i and from the extended equation with the condition (38). The discretization shown in Figure 2(b) is used in these computations, but the number of panels is increased four times to show the better resolution for the fluid velocity on S_b. Figure 7 shows the modulus of the vertical velocity on S_b as a function of z. The velocity is computed at the centroid of

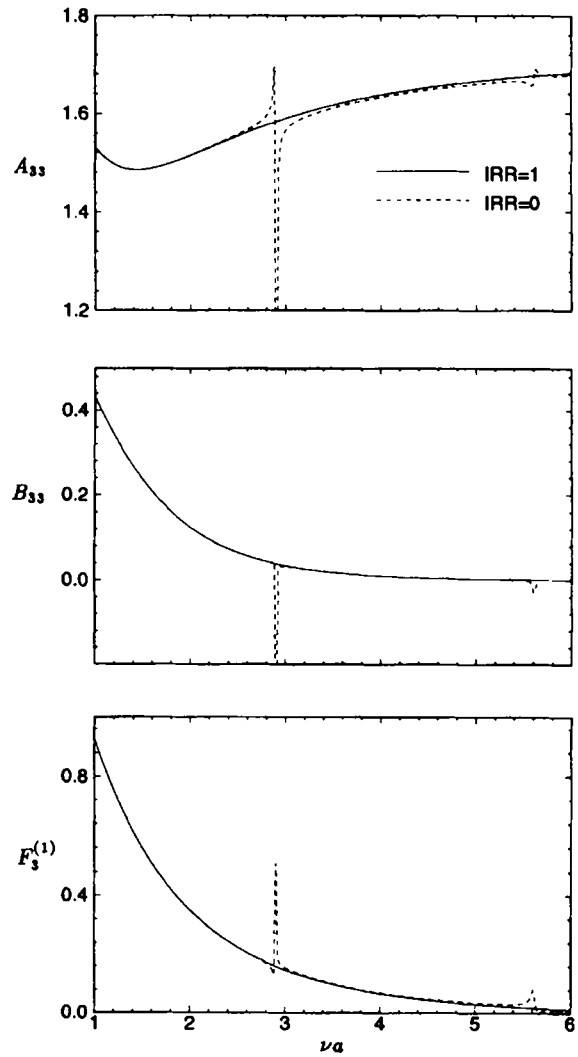

Figure 4. Heave added mass and damping coefficients and modulus of the linear exciting force on the cylinder as functions of νa. Other definitions are given in Figure 3

each panel on the weather side of the cylinder. Here the non-dimensional wave number $\nu a = 2$, where a is the radius of the cylinder. Since this wave number is well below the lowest irregular frequency of the cylinder, near $\nu a = 2{\cdot}88$, the velocity obtained from the unmodified equation is not affected by the irregular frequency. As expected, the vertical (tangential) velocity computed with the homogeneous Neumann condition shows a singular behaviour near the intersection point. The effect of this behaviour of the velocity is reflected in the quadratic force (43) as illustrated in Figure 8, where the surge mean force on the fixed cylinder is presented. The irregular frequency effects are clearly removed using the extended boundary integral equations. However, erroneous results are obtained with the homogeneous Neumann condition. On the other hand, with the appropriate boundary condition (38), the fluid velocity and the mean force agree with the results from the unmodified

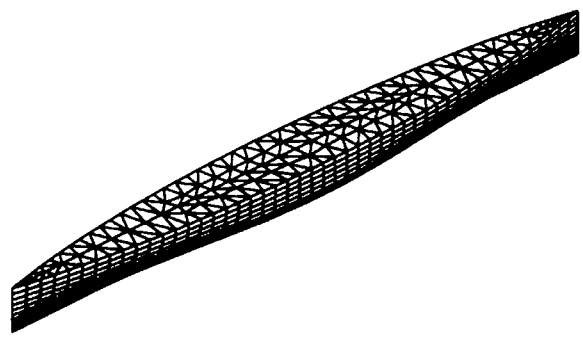

Figure 5. Discretization of Wigley hull and its S_i used in computation

equation away from the irregular frequency. In these computations the velocity potential at the centroid of the panels on S_b adjacent to C_w is substituted into (38) to evaluate $V(\mathbf{x})$. This value of $V(\mathbf{x})$ is assigned on the centroid of the panels adjacent to C_w on S_i and on the centroids of each interior panel along the same radial line.

To illustrate a practical application where the second-order force (41) is important, Figure 10 shows the sum-frequency surge and heave forces and pitch moment acting on Snorre TLP fixed in monochromatic waves. The results from the unmodified and the extended equation with proper Neumann condition on S_i are compared. This platform is shown in Figure 9, where S_b and S_i are discretized with 3488 and 576 panels respectively. The results in Figure 10 show the detrimental effect of the irregular frequency on the prediction of the second-order force when the unmodified equation is used to solve for the first- and second-order potentials. This is due to the high density of irregular frequencies over the relevant sum-frequency range. The surge force is affected by the irregular frequency more than the heave force or the pitch moment. The irregular frequency effects below $va = 2{\cdot}4$ originate from the solution of the integral equations for the second-order problem where the corresponding wave numbers are four times the linear wave numbers shown by the abscissa of Figure 10. The associated wavelength of the homogeneous solutions is shorter than the draft of the TLP. As a result, the heave force and the pitch moment (about the midpoint on the free surface) are affected less than the surge force. On the other hand, the first irregular frequency effect of the linear solution near $va = 2{\cdot}4$ affects the heave force and the pitch moment significantly. (The error in the linear solution affects the second-order solution not only directly in the quadratic force but also indirectly in the evaluation of the forcing functions q_f and q_b.) The forces and moment computed by the combined use of the extended boundary integral equations for the potential and source formulations are free of these irregular frequency effects.

In these numerical examples the required additional unknowns on the interior free surface are relatively small. Thus the additional computational effort due to the increment of the unknowns is not significant. However, we have found that the linear systems associated with the extended boundary integral equations are poorly conditioned in comparison with the corresponding unmodified equation. The FORTRAN subroutine library LINPACK is used to compute the condition number and this is generally an order of magnitude larger for the extended boundary integral equation compared with the unmodified equation. Despite the bad conditioning, the accuracy of the solution is satisfactory as shown in Table I and II, where the surge and heave added-mass and damping coefficients of a floating hemisphere are compared with the corresponding results of Hulme,[22] which are accurate to four significant digits.

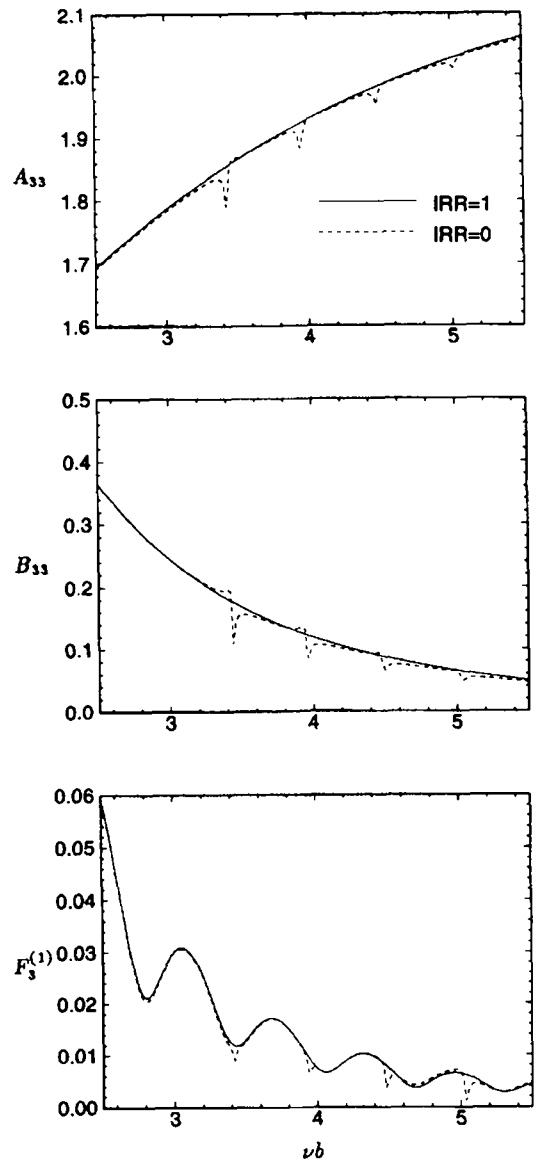

Figure 6. Heave added mass and damping coefficients and modulus of the linear exciting force on the cylinder as functions of νb. Here b is the maximum breadth of the wetted hull. Other definitions are given in Figure 3

On the other hand, the iterative solution procedure for the solution of the linear system, which is generally used for the unmodified equations, does not converge consistently when it is applied to the extended equations. To overcome this problem, it has been necessary to use either Gauss elimination or a block iterative method (typically two to four diagonal blocks), which increases the computational cost.

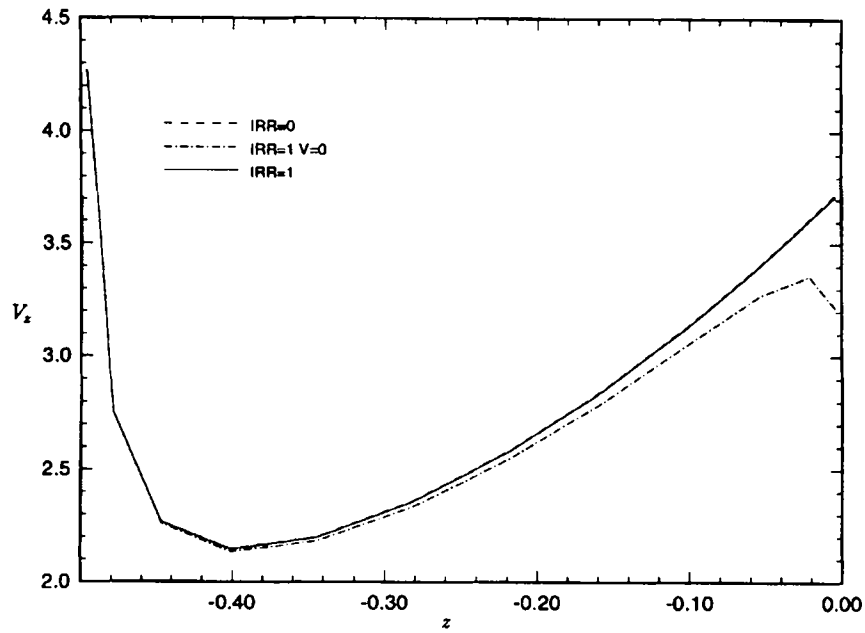

Figure 7. Modulus of the vertical fluid velocity on the cylinder surface as a function of vertical co-ordinate z. The incident wave number is $va = 2$. The velocity is computed on the centroids of a strip of the panels close to the weather side of the cylinder. The velocity is normalized by $igA/\omega a$, where 'i' is the unit imaginary number. Other definitions are given in Figure 3. Comparisons are made between results from the unmodified integral equation (IRR = 0), the extended boundary integral equation with homogeneous Neumann condition (IRR = 1, $V = 0$) and the extended boundary integral equation with the condition (38) (IRR = 1)

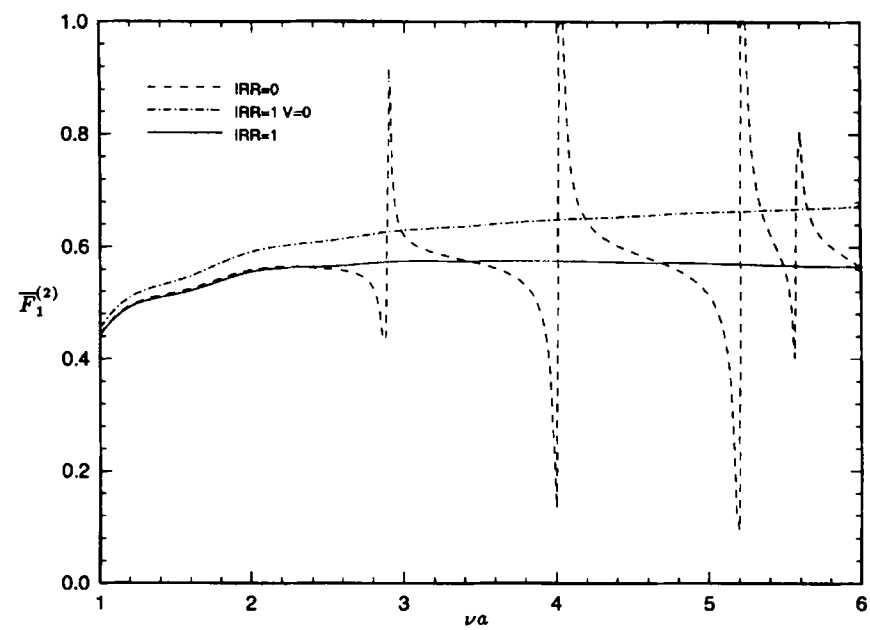

Figure 8. Mean force on the fixed cylinder in the direction of incident wave as a function of va. The force is normalized by $\rho g A^2 a$. Other definitions are given in Figures 3 and 7

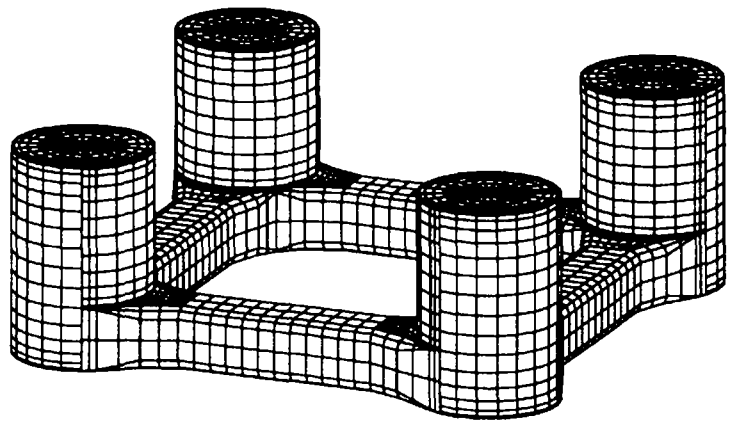

Figure 9. Discretization of Snorre TLP and its S_i

5. CONCLUSIONS

The usual integral equations which are used to analyse wave–body interactions suffer from the presence of irregular frequencies. The detrimental effects on the numerical solution are manifested over the high frequency range owing to the high density of the irregular frequencies, as shown in the example of the second-order sum-frequency wave exciting forces on a TLP.

The extended boundary integral equations are re-examined and extended to remove the irregular frequency effects from the second-order solution as well as from the first-order solution. The velocity potential is obtained from the potential formulation and the fluid velocity from the source formulation. For the latter it is shown that the boundary condition on the interior free surface needs to be specified in terms of the exterior velocity potential to avoid a singularity in the source strength near the waterline. By examining the artificial interior flow which determines the source strength, an appropriate boundary condition is suggested.

The method is found to be effective in removing the effects of irregular frequencies. In particular, the computational results for both first- and second-order hydrodynamic forces are not only free of the irregular frequency effects but also agree well with those from the unmodified integral equations away from the irregular frequencies.

Since our approach to discretizing the integral equations is based on the low-order panel method and we need to evalute the fluid velocity as well as potential on and near the body, we are forced to use both potential and source formulations. An alternative procedure is to use a higher-order panel method where the body geometry and the unknown potential or source strength are approximated by piecewise continuous functions. Maniar[23] has shown that the use of a higher-order panel method based on B-splines also substantially reduces the bandwidth of the irregular frequencies and this approach may be able to provide accurate spatial derivatives on or near the body surface directly from the potential formulation.

ACKNOWLEDGEMENTS

This work was conducted under a Joint Industry Project 'Wave effects on offshore structures' sponsored by Chevron, Conoco Norway, David Taylor Model Basin, Det Norske Veritas, Exxon, Mobil, the Offshore Technology Research Center, the National Research Council of Canada, Norsk Hydro AS, Petrobras, Saga Petroleum, Shell Development Company and Statoil AS. Additional support was provided by the National Science Foundation, Grant 9416096-CTS.

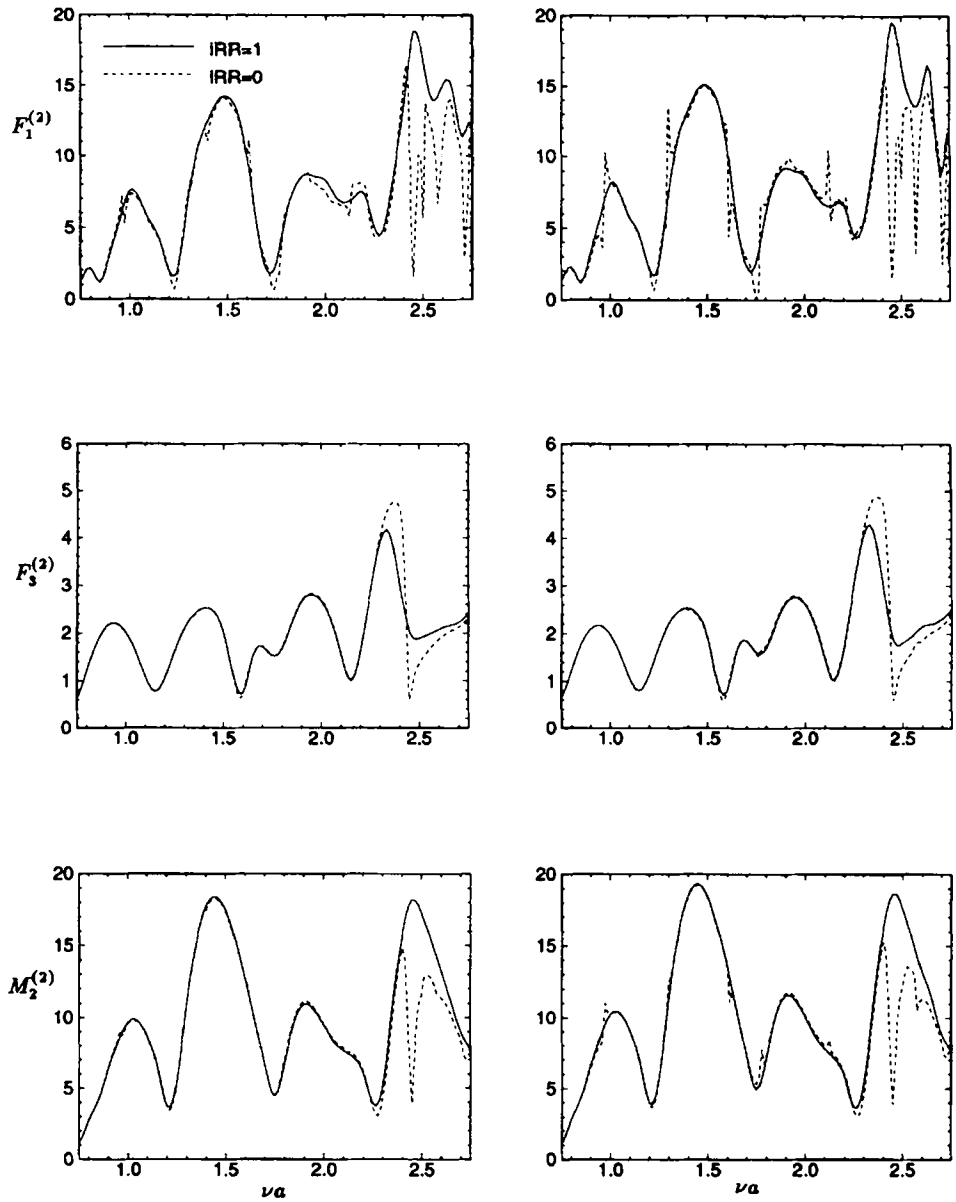

Figure 10. Complete second-order surge and heave forces and pitch moments on fixed Snorre TLP as functions of νR. The forces are normalized by $\rho g A^2 a$ and the moments by $\rho g A^2 a^2$. The results on the left are obtained from the direct approach and those on the right from the indirect approach. Comparisons are made between results from the unmodified integral equation (IRR = 0) and the extended boundary integral equation with the condition (38) (IRR = 1)

Table I. Convergence of surge added-mass and damping coefficients of a floating hemisphere. Three discretizations are used on the body and the interior free surface: 400, 1600 and 6400 panels on the body and 280, 1040 and 4160 panels on the free surface. Each column corresponds to a different discretization with increasing panels from left to right for each coefficient. The last column for each coefficient is the result of Hulme.[22] For each wave number two set of results are presented: the first row is obtained from the unmodified integral equations and the second row from the extended boundary integral equations

va	Added-mass coefficients				va	Damping coefficients			
1·0	1·195	1·200	1·202	1·202	1·0	0·7297	0·7378	0·7399	0·7404
	1·195	1·200	1·202			0·7284	0·7375	0·7398	
2·5	0·4077	0·4085	0·4086	0·4086	2·5	0·5753	0·5788	0·5797	0·5799
	0·4122	0·4096	0·4089			0·5745	0·5786	0·5796	
4·0	0·3765	0·3470	0·3404	0·3393	4·0	0·3003	0·3141	0·3159	0·3165
	0·3428	0·3404	0·3396			0·3153	0·3162	0·3164	
5·0	0·3526	0·3520	0·3517	0·3516	5·0	0·2219	0·2240	0·2246	0·2247
	0·3547	0·3526	0·3519			0·2250	0·2248	0·2247	

Table II. Convergence of heave added-mass and damping coefficients of a floating hemisphere (see Table I for details)

va	Added-mass coefficients				va	Damping coefficients			
1·0	0·8971	0·8974	0·8975	0·8972	1·0	0·5197	0·5201	0·5202	0·5202
	0·8981	0·8976	0·8975			0·5201	0·5203	0·5203	
2·5	0·8151	0·8287	0·8337	0·8352	2·5	0·1363	0·1378	0·1395	0·1412
	0·8430	0·8350	0·8353			0·1434	0·1416	0·1412	
4·0	0·9035	0·9052	0·9054	0·9052	4·0	0·0468	0·0461	0·0459	0·0459
	0·9036	0·9049	0·9053			0·0479	0·0463	0·0459	
5·0	0·9338	0·9361	0·9365	0·9364	5·0	0·0251	0·0244	0·0243	0·0243
	0·9351	0·9361	0·9364			0·0260	0·0247	0·0244	

APPENDIX I: DECOMPOSITION OF THE VELOCITY POTENTIAL

The first- and second-order velocity potentials $\phi^{(1)}$ and $\phi^{(2)}$ are decomposed into the incident wave potentials $\phi_I^{1,2}$, the scattered potentials $\phi_S^{1,2}$ and the radiation potential components ϕ_k as in the following equation:

$$\phi^{1,2} = \phi_I^{1,2} + \phi_S^{1,2} + i\omega \sum_{k=1}^{6} \xi_k^{1,2} \phi_k. \tag{45}$$

The second-order solutions are further decomposed into the sum- and difference-frequency components and distinguished by the superscripts + and − respectively. In (45), ω is not fixed but depends on the component potentials.

The potential $\phi_I^{(1)}$ is defined in (1). The radiation potential components ϕ_k and the first-order scattered potential satisfy the homogeneous free surface condition $q_f = 0$. For ϕ_k the body forcing is $q_b = n_k$, while for $\phi_S^{(1)}$, $q_b = -\partial\phi_I^{(1)}/\partial n$. Here n_k are the Cartesian components of $\mathbf{n}$ and $\mathbf{x} \times \mathbf{n}$ for the translational and rotational modes respectively.

The second-order potentials are subject to the inhomogeneous free surface condition. The free surface forcing q_f is determined by the quadratic interaction of the two first-order solutions ϕ_i and ϕ_j and it takes the form

$$q_f^+ = \frac{i}{4g}\omega_i\phi_i\left(\omega_j^2\frac{\partial\phi_j}{\partial z} + g\frac{\partial^2\phi_j}{\partial z^2}\right) + \frac{i}{4}\omega_j\phi_j\left(-\omega_i^2\frac{\partial\phi_i}{\partial z} + g\frac{\partial^2\phi_i}{\partial z^2}\right) - \tfrac{1}{2}i(\omega_i + \omega_j)\nabla\phi_i \cdot \nabla\phi_j \tag{46}$$

for the sum-frequency component and

$$q_f^- = \frac{i}{4}\omega_i\phi_i\left(-\omega_j^2\frac{\partial\phi_j^*}{\partial z} + g\frac{\partial^2\phi_j^*}{\partial z^2}\right) - \frac{i}{4g}\omega_j\phi_j^*\left(-\omega_i^2\frac{\partial\phi_i}{\partial z} + g\frac{\partial^2\phi_i}{\partial z^2}\right) - \tfrac{1}{2}i(\omega_i - \omega_j)\nabla\phi_i \cdot \nabla\phi_j^* \tag{47}$$

for the difference-frequency component, where a superscript asterisk denotes the complex conjugate. If we consider the interaction between the incident waves only in (46) and (47) and denote them by $q_I^\pm$, the second-order incident wave potential follows from (2) in the form

$$\phi_I^\pm = \frac{q_I^\pm(x, y)e^{\nu_{ij}^\pm z}}{-(\omega_i \pm \omega_j)^2 + g\nu_{ij}^\pm}, \tag{48}$$

where

$$\nu_{ij}^\pm = \sqrt{[(\nu_i\cos\beta_i \pm \nu_j\cos\beta_j)^2 + (\nu_i\sin\beta_i \pm \nu_j\sin\beta_j)^2]}. \tag{49}$$

The free surface forcing for the second-order scattered potential $\phi_S^{(2)}$ is the difference $q_f^\pm - q_I^\pm$. The body forcing for $\phi_S^{(2)}$ is given by $q_b = -\partial\phi_I^{(2)}/\partial n$ when the body is fixed.

APPENDIX II: $\psi(\mathbf{x})$ NEAR THE INTERSECTION POINT

Here we examine the singular behaviour of $\psi(\mathbf{x})$ within small radial distances from C_w compared with the local radius of curvature. The flow is assumed to be locally two-dimensional. We consider only the case where the intersection angle between the body and the free surface is 90°. In the subsequent discussion $\psi(\mathbf{x})$ represents the singular component of the interior potential near the intersection point.

Let $x = 0$ represents the body surface, $y = 0$ the free surface and $x > 0$ and $y < 0$ the interior fluid domain as shown in Figure 11. Let us introduce a new function $\varphi(x, y)$ such that

$$\varphi(x, y) = \psi_y(x, y). \tag{50}$$

Suppose there is a discontinuity of the vertical velocities on S_b and S_i across C_w (i.e. (38) is not satisfied). On $y = 0$ we may simply assume

$$V(x) = \varphi(x, 0) = 0. \tag{51}$$

On $x = 0$, we have the following condition from (27):

$$\varphi(0, y) = \nu\phi(0, 0) \equiv \nu\phi_o, \tag{52}$$

where we consider the first term of the Taylor series expansion of the external velocity potential and utilize the homogeneous free surface condition. The higher-order terms in the Taylor expansion do not contribute to the singular behaviour of the fluid velocity (to leading order) and thus they can be neglected.

The solution of equations (51) and (52) may be obtained in terms of the complex variable $z = x + iy = re^{i\theta}$. Similar technique has been used to analyse the local behaviour of the external flow (see e.g. Reference 24). We introduce a complex potential $F(z)$ and a reduced potential $G(z)$ such that $\psi(x, y) = \mathrm{Re}[F(z)]$ and $\varphi(x, y) = \mathrm{Re}[G(z)]$. We easily find that the solution of (51) and (52) for $G(z)$ is

$$G(z) = \frac{2v\phi_0}{\pi} i \log z. \tag{53}$$

From the equation (50) we find that $F(z)$ is related to $G(z)$ by the equation

$$\frac{dF(z)}{dz} = -iG(z). \tag{54}$$

Consequently, the solution for $F(z)$ is

$$F(z) = -i\int_{z_0}^{z} G(w)dw = \frac{2v\phi_0}{\pi}\int_{z_0}^{z} \log w \, dw. \tag{55}$$

By taking a path along a ray from the origin of the co-ordinate system for the integral in (55) and taking the real part of $F(z)$, we have the velocity potential in the form

$$\psi(x, y) = \frac{2v\phi_0}{\pi} r[\cos\theta(\log r - 1) - \theta \sin\theta]. \tag{56}$$

The normal velocity on $x = 0$ is given by

$$\frac{\partial\psi(0, y)}{\partial x} = \frac{2v\phi_0}{\pi} \log y. \tag{57}$$

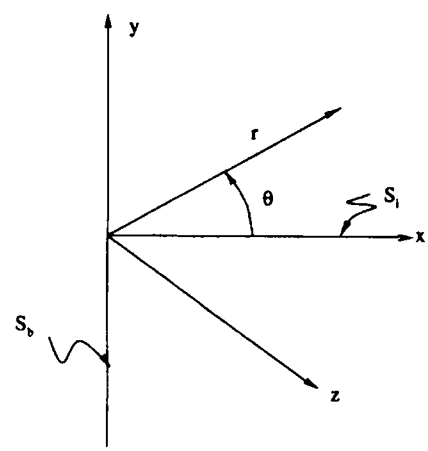

Figure 11. The co-ordinate system

Thus the source strength defined in (31) has a logarithmic singularity near the origin on the body surface. On the free surface near the origin, the source strength is less singular and behaves like $x \log x$.

Next we examine the influence of the singular behaviour of the source strength on the evaluation of the external velocity potential and the tangential fluid velocity on S_b. For this purpose we substitute (57) into σ on S_b in the two dimensional form of equation (30) and its vertical derivative. The integral over S_i can be neglected, since its contribution is dominated locally by the integral over S_b. By similar reasoning we neglect the regular component of the Green function and consider the Rankine source and its image above the free surface. As a result, the behaviour of the velocity potential near C_w is approximated by the integral

$$I(y) = \int^0 \psi_x(0, \eta) G(0, y; 0, \eta) \mathrm{d}\eta = -\frac{2\nu\phi_o}{\pi} \int^0 \log \eta (\log |y^2 - \eta^2|) \mathrm{d}\eta, \tag{58}$$

and that of the vertical fluid velocity by the derivative of (58),

$$\frac{\mathrm{d}I(y)}{\mathrm{d}y} = \int^0 \psi_x(0, \eta) \frac{\partial G(0, y; 0, \eta)}{\partial y} \mathrm{d}\eta = -\frac{2\nu\phi_o}{\pi} \int^0 \left(\frac{\log \eta}{|y - \eta|} - \frac{\log \eta}{y + \eta} \right) \mathrm{d}\eta. \tag{59}$$

It is easy to check that $I(y)$ or the velocity potential is bounded but $\mathrm{d}I(y)/\mathrm{d}y$ or the tangential velocity is unbounded as $y \to 0$. For the latter, the singularity is $O(\log^2 y)$ and its strength is proportional to the difference between the vertical velocities on S_b and S_i. Thus this singularity can be avoided if we impose the condition that the vertical velocity is continuous between the exterior and interior domains.

REFERENCES

1. B. Molin, 'Second order diffraction loads upon three dimensional bodies', *Appl. Ocean Res.*, **1**, 197–202 (1979).
2. H. Lamb, *Hydrodynamics*, Dover, New York, 1932.
3. C.-H. Lee and P. D. Sclavounos, 'Removing the irregular frequencies from integral equations in wave–body interactions', *J. Fluid Mech.*, **207**, 393–418 (1989).
4. S. Ohmatsu, 'On the irregular frequencies in the theory of oscillating bodies in a free surface', *Papers Ship Res. Inst., No. 48*, 1975.
5. R. E. Kleinman, 'On the mathematical theory of the motion of floating bodies—an update', *DTNSRDC-82/074*, 1982.
6. T. F. Ogilvie and Y. S. Shin, 'Integral-equation solution for time- dependent free surface problems', *J. Soc. Naval Archit. Jpn.*, **143**, 86–96 (1977).
7. F. Ursell, 'Irregular frequencies and the motion of floating bodies', *J. Fluid Mech.*, **105**, 143–156 (1981).
8. X. Zhu, 'Irregular frequency removal from the boundary integral equation for the wave–body problem', *M.S. Thesis*, Department of Ocean Engineering, MIT, Cambridge, MA, 1994.
9. A. J. Burton and G. F. Miller, 'The application of integral equation methods to the numerical solution of some exterior boundary-value problems', *Proc. R. Soc. A*, **323**, 201–220 (1971).
10. R. Zhao and O. M. Faltinsen, 'Interaction between current, waves and marine structures', *Proc. 5th Int. Conf. on Numerical Ship Hydrodynamics*, Hiroshima, 1989.
11. J. V. Wehausen and E. V. Laitone, 'Surface waves', in *Handbuch der Physik*, Springer, Berlin, 1960, pp. 446–778.
12. H. A. Schenck, 'Improved integral equation formulation for acoustic radiation problems', *J. Acoust. Soc. Am.*, **44**, 41–58 (1968).
13. S. M. Lau and G. E. Hearn, 'Suppression of irregular frequency effects in fluid–structure interaction problems using a combined boundary integral equation method', *Int. j. numer. methods fluids*, **9**, 763–782 (1989).
14. J. N. Newman, 'Algorithms for the free-surface Green function', *J. Eng. Math.*, **19**, 57–67 (1985).
15. F. John, 'On the motion of floating bodies, II', *Commun. Pure Appl. Math.*, **3**, 45–101 (1950).
16. O. D. Kellog, *Foundations of Potential Theory*, Dover, New York, 1953.
17. F. T. Korsmeyer, C.-H. Lee, J. N. Newman and P. D. Sclavounos, 'The analysis of wave effects on tension-Leg platforms'. Invited paper of OMAE '88 Conf. Houston, TX, 1988.
18. C.-H. Lee, J. N. Newman, M.-H. Kim and D. K. P. Yue, 'The computation of second-order wave loads', *Proc. OMAE Conf.*, Stavanger, 1991.

19. C.-H. Lee and J. N. Newman, 'First- and second-order wave effects on a submerged spheroid', *J. Ship Res,*, **35**, 183–190 (1991).
20. O. M. Faltinsen and A. E. Løken, 'Drift forces and slowly varying horizontal forces on a ship in waves', *Proc. Symp. on Applied Mathematics Dedicated to the Late Prof. Dr. R. Timman*, Delft, 1978.
21. M. J. Lighthill, 'Waves and hydrodynamic loading', *Proc. 2nd Int. Conf. on the Behaviour of Offshore Structures (BOSS '79)*, London, 1979.
22. A. Hulme, 'A ring-source/integral-equation method for the calculation of hydrodynamic forces exerted on floating bodies of revolution,' *J. Fluid Mech.* **128**, 387–412 (1983).
23. H. D. Maniar, 'A three dimensional higher order panel method based on B-splines', *Ph.D. Thesis*, Department of Ocean Engineering, MIT, Cambridge, MA, 1995.
24. P. D. Sclavounos, 'Radiation and diffraction of second-order surface waves by floating bodies', *J. Fluid Mech.*, **196**, 65–91 (1988).